Published in final edited form as:
Dev Biol. 2010 August 15; 344(2): 682–692. doi:10.1016/j.ydbio.2010.05.499.

Mutant DLX 3 disrupts odontoblast polarization and dentin formation

S.J. Choi[a], **I.S. Song**[b], **J.Q. Feng**[c], **T. Gao**[c], **N. Haruyama**[d], **P. Gautam**[a], **P.G. Robey**[a], and **Thomas C. Hart**[a,*]

[a] Craniofacial and Skeletal Diseases Branch, National Institute of Dental and Craniofacial Research, National Institutes of Health, Bethesda, MD, USA

[b] Asan Institute of Life Sciences, Laboratory of National Investment Project, Dept. of Rheumatology, Ulsan University Medical School, Seoul, Republic of Korea

[c] Biomedical Sciences, Baylor College of Dentistry, Texas A&M Health Science Center, Dallas, TX, USA

[d] Department of Maxillofacial Orthognathics, Tokyo Medical and Dental University Graduate School, Tokyo, Japan

Abstract

Tricho-dento-osseous (TDO) syndrome is an autosomal dominant disorder characterized by abnormalities in the thickness and density of bones and teeth. A 4-bp deletion mutation in the Distal-Less 3 (*DLX3*) gene is etiologic for most cases of TDO. To investigate the in vivo role of mutant DLX3 (MT-DLX3) on dentin development, we generated transgenic (TG) mice expressing MT-DLX3 driven by a mouse 2.3 Col1A1 promoter. Dentin defects were radiographically evident in all teeth and the size of the nonmineralized pulp was enlarged in TG mice, consistent with clinical characteristics in patients with TDO. High-resolution radiography, microcomputed tomography, and SEM revealed a reduced zone of mineralized dentin with anomalies in the number and organization of dentinal tubules in MT-DLX3 TG mice. Histological and immunohistochemical studies demonstrated that the decreased dentin was accompanied by altered odontoblast cytology that included disruption of odontoblast polarization and reduced numbers of odontoblasts. TUNEL assays indicated enhanced odontoblast apoptosis. Expression levels of the apoptotic marker caspase-3 were increased in odontoblasts in TG mice as well as in odontoblastic-like MDPC-23 cells transfected with MT-DLX3 cDNA. Expression of *Runx2*, *Wnt 10A*, and *TBC1D19* colocalized with DLX3 expression in odontoblasts, and MT-DLX3 significantly reduced expression of all three genes. TBC1D19 functions in cell polarity and decreased *TBC1D19* expression may contribute to the observed disruption of odontoblast polarity and apoptosis. These data indicate that MT-DLX3 acts to disrupt odontoblast cytodifferentiation leading to odontoblast apoptosis, and aberrations of dentin tubule formation and dentin matrix production, resulting in decreased dentin and taurodontism.

In summary, this TG model demonstrates that MT-DLX3 has differential effects on matrix production and mineralization in dentin and bone and provides a novel tool for the investigation of odontoblast biology.

* Corresponding author. National Institutes of Health, Building 30, RM 524, 30 Convent Drive, Bethesda, MD 20892, USA. Fax: +1 301 480 2055. thart@mail.nih.gov (T.C. Hart)..

Appendix A. Supplemental data

Supplementary data associated with this article can be found, in the online version, at doi:10.1016/j.ydbio.2010.05.499.

Keywords

DLX3; Transgenic mouse; Dentin mineralization; Taurodontism, TDO, odontoblast polarization; apoptosis, TBC1D19

Introduction

Distal-less 3 (DLX3) mutations are etiologic for tricho-dento-osseous (TDO) syndrome, an autosomal dominant condition characterized by anomalies in hair, teeth, and bone (OMIM190320). The most common form of TDO is due to a c.571_574delGGGG mutation in *DLX3* (Price et al., 1998a, 1998b). Affected individuals have kinky, curly hair at birth, dental anomalies consisting of thin enamel, thin dentin, taurodontism, and an increased thickness and density of bone (Wright et al., 1997; Haldeman et al., 2004; Islam et al., 2005). Studies have evaluated normal and mutant DLX3 function in hair (Duverger et al., 2008; Hwang et al., 2008; Di Costanzo et al., 2009) and bone (Choi et al., 2008, 2009; Li et al., 2008; Hassan et al., 2009) development, but the in vivo effect of mutant *DLX3* on dentin mineralization and tooth development is less well studied. In TDO, mutant DLX3 is associated with increased bone thickness and density but decreased thickness of dentin, indicating a differential mode of action in disrupting development of these two mineralized tissues. In vitro analyses of mineralizing cells including ameloblasts, chondrocytes, odontoblasts, and osteoblasts have shown that the temporal expression of the DLX3 homeoprotein varies specifically according to the terminal differentiation for each cell type, suggesting cell specificity in DLX3 function (Ghoul-Mazgar et al., 2005).

To characterize the in vivo effect of mutant *DLX3* on dentin development, we performed in vivo and in vitro studies of transgenic (TG) mice with the c.571_574delGGGG *DLX-3* deletion mutation (MT-DLX3) driven by a mouse 2.3 Col1A1 promoter. We observed reduced dentin formation in TG mice was associated with disruption of odontoblast cytodifferentiation and increased odontoblast apoptosis. To understand the molecular factors disrupting dentin development, we studied the effect of MT-DLX3 on odontoblast polarization and secretion of dentin matrix proteins. As odontoblast polarization requires signaling through Frizzled receptors (Axelrod et al., 1998) and Wnt10A is required for normal odontoblast differentiation and secretion of the primary dentin matrix protein (DSPP) (Yamashiro et al., 2007), we evaluated the expression of Wnt10A and Tre-2/Bub2/Cdc16 (TBC)1 domain family, member 19 (TBC1D19), a GTPase activated protein reported to function in cell polarity (Zhang et al., 2005). Here we report that disruption of normal dentin development driven by MT-DLX3 expression occurs due to disruption of odontoblast polarization and increased odontoblast apoptosis, which disrupt normal odontoblast development and secretion of dentin matrix leading to reduced production of dentin.

Materials and methods

Generation of MT-DLX3 TG mice

MT-DLX3 TG mice were generated as described previously (Choi et al., 2009). All experiments were performed under an animal study protocol approved by the NIDCR/NIH Animal Care and Use Committees. Briefly, a full-length mutant DLX3 (MT-DLX3) cDNA with a 4-bp deletion mutation (Choi et al., 2008) was cloned into a pBS KS II vector (Stratagene, La Jolla, CA) containing the 2.3 Col1A1 promoter and injected in to the pronuclei of fertilized FVB mouse oocytes and implanted into pseudopregnant recipients. Positive founders for the MT-DLX3 transgene were bred with wild type mice maintained in FVB background to generate hemizygotes. All mice were fed a soft diet since tooth defects were present in TG mice.

High-resolution radiography and microcomputed tomography (μCT)

Procedures for jaw sample preparation and high-resolution radiology were described previously (Feng et al., 2006; Lu et al., 2007). Briefly, 6-week-old male TG and control mice were euthanized using compressed 5% CO_2 gas, and the cranium was removed, skinned, and fixed with 4% buffer-saturated paraformaldehyde for 48 hours. High-resolution radiography of cranial bones and teeth was performed with a Faxitron MS-20 Radiography System for 90 s at 18 kV (Faxitron X-Ray Lincolnshire, IL) and X-OMAT Kodak diagnostic film (Kodak, Rochester, NY). To examine three-dimensional tooth structures, the craniofacial complex was scanned by an eXplore Locus SP microcomputed (uCT) system (GE Healthcare, London, Canada). The isotropic resolution of the instrument was 10 μm, and the isosurface was reconstructed using two-dimensional raw data and MicroView analysis software (GE Healthcare). The image analysis method was based on Hounsfield units (2800 units) and region-grow algorithms to segment the image data defining the separate anatomic structures studied. Hydroxyapatite equivalent dentin and enamel mineral densities (mg HA/cc) were measured by the eXplore Locus SP μCT software using a 10×10×10 pixel region of interest (ROI) from mandibular first molars from 10 TG and control mice.

Electron microscopy

Scanning electron microscopic (SEM) imaging studies of resin-cast teeth were performed as described previously (Feng et al., 2006; Lu et al., 2007). Mandibles were dissected, fixed in 2% paraformaldehyde and 2.5% glutaraldehyde in 0.1 M cacodylate buffer solution (pH 7.4) at room temperature for 4 hours and then transferred to 0.1 M cacodylate buffer solution. The tissue specimens were dehydrated in ascending concentrations of ethanol, embedded in methyl-methacrylate (Buehler, Lake Bluff, IL), and surface-polished using aluminum alpha micropolish II solution (Buehler) in a soft cloth rotating wheel. The surface was acid etched with 37% phosphoric acid for 2–10 seconds, followed by 5% sodium hypochlorite treatment for 5 minutes. The specimens were then coated with gold and palladium as described previously (Martin et al., 1978). For backscattered SEM, the surface of methyl-methacrylate embedded jaws were polished and then coated with carbon. Specimens were examined with a FEI/Philips XL30 Field emission environmental SEM (Philips, Hillsboro, OR).

Histological and immunohistochemical analysis of teeth

To examine dentin and pulp, standard histological and immunohistochemical analyses were performed as described previously (Choi et al., 2009). Deparaffinized and rehydrated tooth sections were incubated with the specific primary antibodies diluted in Antibody Diluent (559148; BD Biosciences, Franklin Lakes, NJ) and incubated with HRP-conjugated SuperPicture™ Polymer as secondary antibodies (DAB anti-Rabbit; 87-9263 and DAB anti-Goat; 87-9363, Zymed Lab), followed by a DAB coloring reaction. For the detection of WT- and MT-DLX3, slides were incubated with pepsin (Digest-All, 00-3006, Zymed Lab) at 37 °C for 10 min for antigen retrieval, and primary antibodies were incubated on tooth sections as follows: WT-DLX3-specific antibody (sc-18143, 1:20; Santa Cruz Biotechnology, Santa Cruz, CA) and MT-DLX3-specific antibody (1:400) (Choi et al., 2009). To investigate the expression of dentin matrix proteins, Col1A1 antibody (ab765p, 1:100; Chemicon, Billerica, MA), dentin sialophosphoprotein (DSPP and DSP) antibody (LF-153,1:100), biglycan (Bgn) antibody (1:100), and decorin (Dcn) antibody (1:100) (all three antibodies were kindly provided by Dr. Larry Fisher, NIDCR/NIH) were incubated with tooth sections from TG mice and control mice. To investigate the structure of odontoblast primary cilium, we used an acetylated α-tubulin antibody (ab 24610, clone 6-11B-1, 1:100; Abcam, Cambridge, MA) followed by the DAB coloring reaction as described above.

mRNA expression levels of dentin matrix proteins, Runx2, Wnt10A, and TBC1D19 in odontoblast-like MDPC-23 cells and osteoblastic MC3T3E1 cells

Exponentially growing odontoblast-like MDPC-23 cells (2×10^5) derived from fetal mouse molar dental papilla (Hanks et al., 1998)in DMEM containing 10% FBS were plated into six-well plates 24 hours before transfection and then transfected with 2 μg of WT-, MT-DLX3 cDNA, or pcDNA3.1/Hygro (+) empty vector (EV) using the Lipofectamine 2000 kit (Invitrogen, Carlsbad, CA). Green fluorescence protein (GFP) vector was used as a transfection efficiency control. Twenty-four hours after transfection, cells were treated with 100 μg/ml of Hygromycin B (10687010; Invitrogen) for 2 weeks, and single-cell colonies were isolated as described previously (Choi et al., 2008). Established MDPC-23 and MC3T3E1 cells (5×10^4 cells/well in 1 ml of DMEM medium) stably transfected with WT-DLX3, MT-DLX3, or EV were plated on 6-well plates for real-time RT–PCR analysis (Choi et al., 2008). At day 3, cells were lysed in RNAzol (Invitrogen), and total RNA was isolated. Real-time RT–PCR was performed using mouse Col1A1 (QT00162204), DSPP (QT01534568), Bgn (QT00108682), Dcn (QT00131068), Runx2 (QT00102193), osteocalcin (QT00259406), Wnt10A (QT00110089), caspase-3 (QT01164779) QuantiTect Assay primers (Qiagen, Valencia, CA), and SBYR Green dye (204052, Qiagen). mRNA expression levels of TBC1D19 were examined by semiquantitative RT–PCR using total RNA from odontoblast-like MDPC-23 cells and MC3T3E1 cells stably transfected with WT-, MT-DLX3, or EV (TBC1D19 specific primer sets; SS: 5′-ATG CTG TTT TCT ATC CGC CC-3′ and AS: 5′- CCT CGA AGA TCA GGT GAC GG-3′). To investigate the effects of WT- and MT-DLX3 on TBC1D19 promoter activity, we performed TBC1D19 promoter luciferase reporter assays. The distal 1.7 kbp TBC1D19 promoter was amplified using a specific primer set (SS at −1717 nt; 5′-GAT GGC AGG TGT CCA ATC TC-3′ and AS at +160 nt of NM_144517; 5′-GAG CAT ACA AAT TGG AGC CC-3′) and cloned into a pGL2E luciferase reporter vector (Promega, Madison, WI). The TBC1D19 promoter reporter construct was transfected into odontoblast-like MDPC-23 cells and MC3T3E1 cells stably transfected with WT-, MT-DLX3, or EV in the presence of a tkRenilla luciferase construct as an internal transfection control. Promoter activities were measured using a dual luciferase assay kit (Promega). To investigate the effect of TBC1D19 on caspase-3 expression in odontoblasts, siRNAs against TBC1D19 (SI00827827, SI00827834, and SI00827841; Qiagen Co) were transiently transfected into odontoblast-like MDPC-23 cells stably transfected with DLX3 constructs and the mRNA expression levels of caspase-3 were examined real-time RT–PCR as described above.

In situ hybridization of RunX2, Wnt10A, and TBC1D19

Nonradioisotopic in situ hybridization was performed using DIG-labeled cRNA probes (Assmann et al., 1992). Specific primers for amplification of runt-related transcription factor 2 (Runx2) (from 491 to 1291 nt of NM_009820), Wingless-type MMTV integration site family, member 10A (Wnt10A) (from 1801 to 2360 nt of NM_009518), and Tre-2/Bub2/Cdc16 (TBC)1 domain family, member 19 (TBC1D19) (from 1021 to 1801 nt of NM_144517) were designed. Amplified PCR products for Runx2, Wnt 10A, and TBC1D19 were generated from mouse bone marrow cDNA and cloned into the pCR®II-TOPO® vector (Invitrogen). Identity and orientation of the Runx2, Wnt10A, and TBC1D19 cDNAs were verified by direct sequencing. Amplified PCR products downstream of the SP6 promoter for anti-sense probes and T7 promoter for sense probes were generated. Digoxigenin-labeled cRNA probes for Runx2, Wnt10A, and TBC1D19 were prepared with an RNA Labeling Kit (Roche Applied Science, Indianapolis, IN) according to the manufacturer's protocol. Slide mounted tooth sections were hydrolyzed with 10 μg/ml of proteinase K in pH 7.5 Tris buffer, fixed in 4% paraformaldehyde (PFA), treated with 0.2 M HCl, and acetylated in 0.1 M triethanolamine (TEA) containing 0.25% acetic anhydride. Slides were then probed with 110 μl of hybridization buffer (50% formamide, 0.3 M NaCl, 10 mM Tris–HCl pH 7.5, 10

mM Na_2HPO_4 pH 6.8, 1× Denhardt's solution, 1 mg/ml t-RNA, 5 mM EDTA, 10% dextran sulphate) containing DIG-labeled cRNA probes for Runx2, Wnt10A, or TBC1D19 and incubated at 42 ° C for 16 hours. Nonhybridized probe was removed by saline sodium citrate (SSC) buffer washes. For immunodetection of DIG, slides were incubated with blocking buffer containing alkaline phosphatase-conjugated anti-DIG antibodies (Roche, 1:1000) and reacted with NBT/BCIP (Roche) in detection buffer (20 μl NBT/BCIP stock in 1-ml buffer of 100 mM Tris pH 9.5, 100 mM NaCl, 50 mM $MgCl_2$).

Results

Three founder lines were generated and analyzed. As each independent line rendered similar results, the typical, most illustrative images are shown, analyzed, and compiled into relevant tables and figures below.

Radiography and uCT study

High-resolution radiographic analysis of heads from 6-week-old TG mice and control mice revealed that the total anteroposterior lengths of the cranium in TG mice were shorter than those in control mice and the cranium of TG mice appeared more rounded in shape when viewed laterally (Figs. 1a and h). Both mandibular and maxillary incisors displayed increased curvature towards the palate in TG mice, and the lengths of TG mouse maxillary incisors are smaller than those of control mouse (4.22±0.28 mm (TG) versus 5.7±0.41 mm (Con), means±SD, $P<0.005$). The mandibular incisors show a midline diastema and opaque color in TG mice (Fig. 1b), and the length of mandibular incisor is also reduced (6.55±0.27 mm (TG) versus 8.33±0.11 mm (con), means±SD, $P<0.0005$). Radiographically, the amount of dentin appears visibly reduced in molars and incisors from TG mice (Figs. 1a and c). Calculation of the dentin and enamel mineral densities in ten 6-week-old mandibular first molar teeth were not significantly different for TG and control teeth. Dentin mineral density (mean±SD, mg/HA/cc): control: 1232.61±94.86; TG: 1201.78±72.22). Enamel mineral density (mean±SD, mg/HA/cc): control (1956.66±92.97) and TG (1931.07±90.08). The thickness of coronal mineralized tooth structure appears reduced and the size of pulp chambers appear enlarged in molars from TG mice (Figs. 1c and g). μCT studies using optical sectioning of incisors also reveal enlarged pulps in incisors from TG mice as indicated by arrowheads (Figs. 1d and e). Measurement of the thickness of dentin at mesial and distal locations beneath the cemento-enamel junction of mandibular first molars (indicated by red bars; Figs. 1g and n) reveals reduced dentin thickness (0.0838±0.0277 mm (TG) versus 0.2175±0.0306 mm (control), means±SD, $P<0.005$) in TG mice. However, the length of mandibular first molar is not significantly changed in TG mice (2.1717±0.0977 mm (TG) versus 2.2400±0.1166 mm (control), means±SD, P=0.1382). Interestingly, second molars in 50% of TG mice had 6 cusps compared to 5 cusps present in control mice as indicated by a red arrow (Fig. 1f). Analysis of the dentition of 6-month-old mice revealed fracture of enamel from the underlying dentin resulting in a loss of mineralized tooth structure with exposure of the dental pulp in approximately half of the TG mice.

Histological and immunohistochemical analyses of dentin mineralization

To examine tooth structure, dentin, and odontoblast morphology in teeth from TG mice, histological analysis was performed using tooth sections from new born, 14-day-, and 6-week-old male TG and control mice. As shown in Fig. 2a, the cytology of the pulp and dentin structures in new born TG mice were not different from control mice (Fig. 2g). The palisade appearance of polarized odontoblasts and ameloblasts in newborn TG mice (E18.5) were similar to those in control littermates (Figs. 2b and h). In contrast to the palisade appearance of the odontoblasts seen in control odontoblasts at 14 days (Fig. 2J), the odontoblast layer was disrupted and disorganized in the 14-day-old TG mice (Fig. 2d) and

the dentin was visibly thinner in TG mice (Fig. 2c) compared to controls (Fig. 2i). This pattern of disruption of the palisade appearance in the odontoblast layer directly underneath mineralized dentin was more apparent at 6 weeks (Fig. 2f). The number of odontoblasts adjacent to the mineralized dentin layer was visibly reduced in 6-week-old TG mice (Fig. 2f) compared to control sections (Fig. 2l), and high-power magnification revealed the nuclei of some odontoblasts in TG sections were not oval-shaped and apoptotic bodies (indicated by green arrow heads) were visible in the odontoblast layer from TG teeth (Fig. 2f). In addition, the dentin was visibly thinner in TG specimens at 6 weeks (Fig. 2e) compared to controls (Fig. 2k). Similarly, dentin deposition was markedly reduced, and odontoblast polarization was disrupted at 6 weeks in TG mandibular incisors (Figs. 2m and n) compared to controls (Figs. 2p and q). The ameloblast layer in TG incisor sections (Fig. 2o) did not show the same disruption as the odontoblast layer (Fig. 2n) and appeared comparable to control sections (Fig. 2r). High-power magnification revealed disruption in the columnar alignment of odontoblasts, disruption in the characteristic eccentric nuclear localization in the basal aspect of the cell, the presence of apoptotic bodies, and markedly reduced dentinal tubule formation in both molars and incisors from TG mice at 6 weeks (Figs. 2f and n).

Microstructure of dentin and enamel by scanning electron microscopy

To investigate the microstructure of dentin, dentinal tubules, and enamel, we performed backscattered and resin cast scanning electron microscopy. As shown in Figs. 3a and d, the thickness of dentin in both the coronal areas and in the root in the first mandibular molar appears reduced in 6-week-old TG mice, consistent with the histological findings (Figs. 2e and k). Findings from backscattered SEM reveal fewer dentinal tubules in TG dentin (Fig. 3b) adjacent to the dental–enamel junction compared to control dentin (Fig. 3e). Findings from resin cast SEM of the dentin adjacent to the pulp show that in TG dentin (Fig. 3c), there are fewer dentinal tubules, and the orientation of the tubules present is more irregular and disorganized compared to dentin from control mice (Fig. 3f).

The structure of enamel rods and the thickness of the enamel layer of TG mice are not different from those of control mice (Figs. 3b and e).

Expression of dentin matrix proteins

As secretion of the organic matrix is necessary for normal dentin formation, we evaluated the expression patterns of the dentin matrix proteins: dentin sialophosphoprotein (DSPP); collagen type 1, α-1 (Col1A1); biglycan (Bgn); and decorin (Dcn). As shown in Figs. 4l and q, DSPP is expressed in the odontoblast layer and dentinal tubules in control mice. DSPP expression was not seen in the mandibular bone. High-power magnification shows that DSPP expression in TG mice (Fig. 4g) was also seen in the odontoblast layer and in the region containing dentin and dentin tubules, but the expression pattern was less uniform than in corresponding control dentin. Col1A1 was detected in the dentin matrix and mandibular bone in both TG mouse and control mouse sections (Figs. 4c and m). High-power magnification shows that Col1A1 is mainly detected in the dentin in both TG and control sections, but the pattern of Col1A1 staining appears less organized in the TG sections (Fig 4h) compared to control mice (Fig. 4r). Biglycan was expressed in control dentin (Fig. 4s), and the distribution was similar in the odontoblast layer as well as the region containing the predentin and dentin. In TG sections (Fig. 4i) biglycan expression appeared in the odontoblast layer, and expression was greater in the predentin layer, and less in the dentin that would contain dentinal tubules compared to controls. Decorin was expressed in both the odontoblast layer as well as in the predentin and dentin layers, in control specimens (Fig. 4t) Decorin was expressed in the odontoblast layer in high-power magnification of TG section (Fig. 4j), but its expression appeared less in the area that contains dentin and dentin tubules.

To investigate the expression levels of these dentin matrix proteins in odontoblast-like MDPC-23 cells, we performed real-time RT–PCR. As shown in Fig. 4B, mRNA expression levels of DSPP and Bgn were increased by WT-DLX3 compared to those of EV-transfected cells. However, MT-DLX3 did not significantly alter DSPP and Bgn mRNA expression compared to WT-DLX3. mRNA expression levels of Col1A1 and Dcn did not appear changed by WT- or MT-DLX3 compared to those of EV-transfected cells (Fig. 4B).

Apoptosis of odontoblasts and expression of apoptotic markers

Findings from histochemical, radiographic, and SEM analyses indicated that, in TG mice, the dentin layer was thinner, the number of odontoblasts was reduced, and apoptotic bodies were present in the odontoblast layer (Figs. 2f and n). To investigate whether odontoblast apoptosis could contribute to these findings, we evaluated the expression of the apoptotic markers TUNEL and caspase-3 in odontoblasts from tooth sections at different stages of development including newborn, 14 days, and 6 weeks. We found no differences in the presence of TUNEL-positive cells or caspase-3 expression for tooth sections at the newborn stage (data not shown) or at 14 days (Figs. 5a. and g; and Supplemental Fig. 2). As shown in Figs. 5b and c, TUNEL-positive cells (brown signal) were seen in the differentiated odontoblasts adjacent to the mineralized dentin in 6-week-old TG mice, while TUNEL-positive cell is not found in tooth sections of 6-week-old control mice (Figs. 5h and i). High-power magnification shows the nuclear localization of the TUNEL staining signal in TG odontoblasts (Fig. 5c). TUNEL staining signal was not detected in bone cells from either TG (Fig. 5d) or control (Fig. 5j) sections. Caspase-3 staining was also positive in the cytosol of differentiated odontoblasts from TG mice at 6 weeks (Figs. 5e and f) but not in the tooth sections from control mice (Figs. 5k and l). Caspase-3 staining was not detected at the newborn or at 14 days and was not detected in bone at the newborn, 14-day, or 6-week stages (data not shown).

To determine if there may be a cell-specific propensity for apoptosis, we examined the effect of MT-DLX3 on the expression levels of apoptotic markers in odontoblast-like MDPC-23 cells and MC3T3E1 cells. Findings of these in vitro studies showed that MT-DLX3 significantly increased the expression levels of caspase-3 mRNA in odontoblast-like MDPC-23 cells (Fig. 5m) but not in preosteoblastic MC3T3E1 cells (Fig. 5n). mRNA expression levels of caspase-3 were not changed in those cells stably transfected with WT-DLX3 cDNA compared to those of empty vector (EV)-transfected cells. The number of TUNEL-positive cells was also increased in MDPC-23 cells transfected with MT-DLX3 in the presence of mineralization media (Fig. 5o).

WT-DLX3, MT-DLX3, Runx2, Wnt10A, TBC1D19, and acetylated α-tubulin expression in odontoblasts

To determine downstream targets of MT-DLX3, we examined the expression patterns of WT-DLX3 and MT-DLX3 proteins as well as *Runx2*, *Wnt10A*, and *TBC1D19* mRNA in differentiated odontoblasts since these molecules are important for odontoblast polarization and differentiation and dentin formation (Zhang et al., 2005; Yamashiro et al., 2007; Bohring et al., 2009). As shown in Fig. 6, expression of WT-DLX3 protein was detected in preodontoblasts, differentiated odontoblasts and osteoblasts but not in pulp cells of the 14-day-old mandibular first molar sections from TG and control mice (Figs. 6b, ba, bb, j, ja, and jb), while MT-DLX3 protein expression was observed in these cells including pulp cells from TG mice (Figs. 6c, ca, and cb). *Runx2* mRNA expression was reduced in differentiated odontoblasts but not in osteoblasts and osteocytes of TG mice (Figs. 6d, da, and db) compared to controls (Figs. 6l, la, and lb). mRNA expression of *Wnt10A* (Figs. 6e and ea) and *TBC1D19* (Figs. 6f and fa) were also reduced in odontoblasts in TG mice compared to controls (*Wnt10A*: Figs. 6m and ma; *TBC1D19*: Figs. 6n and na). *Wnt10A* mRNA expression

was not reduced in osteoblasts in TG mice compared to controls (Figs. 6eb and mb). *TBC1D19* mRNA was not expressed in bone cells in either TG or control mice (Figs. 6fb and nb). The expression patterns of *Runx2*, *Wnt10A* and *TBC1D19* mRNA colocalized with WT-DLX3 protein expression in odontoblasts adjacent to the mineralized dentin matrix of control mice (Figs. 6la, ma, and na). However, mRNA expression levels of *Runx2*, *Wnt10A*, and *TBC1D19* were reduced in odontoblasts from TG mice in which MT-DLX3 was highly expressed (Figs. 6da, ea, and fa). Immunohistochemical study using an acetylated α-tubulin antibody staining ciliary microtubules (Thivichon-Prince et al., 2009) reveals that the primary cilium structure of odontoblasts in TG mice appears disrupted, with loss of the longitudinal orientation seen in odontoblasts of control mice (Fig. 6p), consistent with disruption of normal odontoblast polarity (Figs. 6g and h).

Effects of MT-DLX3 on TBC1D19, Runx2, and Wnt10A mRNA expression

To evaluate how cell specificity may influence the effects of WT-DLX3 and MT-DLX3 on the expression of *TBC1D19*, *Runx2* and *Wnt10A*, we evaluated their expression in odontoblast-like MDPC-23 cells and preodontoblast-MC3T3E1 cells. RT–PCR studies determined that TBC1D19 was not expressed in osteoblastic MC3T3E1 cells (data not shown). We then measured the promoter activity and mRNA expression levels of TBC1D19 in odontoblast-like MDPC-23 cells. Dual luciferase reporter assays demonstrated that MT-DLX3 down-regulated the 1.7-kbp mouse TBC1D19 promoter activity approximately 4-fold in odontoblast-like MDPC-23 cells compared to those of empty vector (EV) transfected cells, while TBC1D19 promoter activity was not changed in WT-DLX3 transfected cells (Fig. 7a). There are 11 potential DLX3 binding motifs in the 1.7-kbp distal TBC1D19 promoter region used in these experiments. Semiquantitative RT–PCR analysis also revealed that MT-DLX3 reduced TBC1D19 mRNA expression in these cells (Fig. 7b). Runx2 mRNA expression levels were significantly increased in MDPC-23 cells transfected with WT-DLX3 and significantly decreased in these cells transfected with MT-DLX3 (Fig. 7c). In contrast, Runx2 expression levels were increased in MC3T3E1 cells transfected with WT-DLX3 (Fig. 7d) and further increased in these cells by MT-DLX3. Transfection with MT-DLX3 significantly decreased Wnt10A mRNA expression levels in MDPC-23 cells (Fig. 7e), but Wnt10A expression was not significantly change in MC3T3E1 cells (Fig. 7f). However, we could not detect the direct modulatory effects of MT-DLX3 on either Runx2 or Wnt10A promoter activity in odontoblast-like MDPC-23 cells transduced with MT-DLX3 (data not shown). To investigate the effects of TBC1D19 on caspase-3 expression, we performed knockdown experiment using siRNA against TBC1D19. As shown in Fig. 7g, transfection of siRNA against TBC1D19 dramatically increased caspase-3 mRNA expression (90-fold) compared to control transfection with scramble siRNA.

Discussion

DLX3 is important in controlling matrix deposition and biomineralization, but its effect on mineralized tissue development may be cell specific(Beanan and Sargent, 2000, Hassan et al., 2004, Ghoul-Mazgar et al., 2005; Li et al., 2008). Cell-specific differences in how DLX3 acts could account for the clinical differences in bone and dentin associated with DLX3 mutations in TDO, where bone matrix apposition and mineralization increase, while the amount of tooth dentin is decreased. These findings are consistent with a cell-specific manifestation of mutant DLX3. In vitro and ex vivo studies indicate that MT-DLX3 acts to increase osteoblast differentiation and osteoblastic calcium deposition (Choi et al., 2008), and in vivo studies of MT-DLX3 TG mice also suggest a novel role in osteoclast differentiation and bone resorption mediated by IFN-γ. Increased expression of IFN-γ by immune cells has been associated with decreased osteoclastic bone resorption, contributing to enhanced trabecular bone volume and mineral density in MT-DLX3 TG mice (Choi et al.,

2009). Findings from the current study indicate that MT-DLX3 has different in vivo effects on odontoblasts compared to osteoblasts and MT-DLX3 disrupts dentin matrix deposition and ultimately dentin formation through a fundamentally different mechanism than its action in bone.

At 6 weeks, MT-DLX3 TG mice demonstrated enlarged pulp chambers and reduced thickness of dentin (taurodontism) similar to clinical characteristics of patients with TDO syndrome. Electron microscopy studies show that the thin dentin layer in TG teeth contains dentinal tubules that are poorly developed, disorganized, and reduced in number. Whereas dentin development was disrupted in this TG mouse model, the enamel appeared to be largely unaffected in terms of the amount and mineral density of enamel produced, although increased enamel porosity adjacent to the DEJ was observed (Supplemental Fig. 1). Although MT-DLX3 is not expressed in ameloblasts in TG mice since the Col1A1 promoter is not expressed in ameloblasts, the altered rod-sheath morphology of the mineralized enamel near the DEJ seen in SEM studies suggest that MT-DLX3 may disrupt the normal signaling between the epithelial ameloblasts and the mesenchymal odontoblasts (Thesleff et al., 1995; Luukko et al., 2005). Altered cusp patterning in the second molars of approximately 50% of the TG mice was also noted, with some TG second molars exhibiting a 6-cusp pattern in contrast to the 5-cusp pattern seen in the controls. While the basis for this altered patterning is unclear, members of the DLX gene family and DLX3 specifically are known to be important in patterning (Weiss et al., 1998; Depew et al., 2005; Lezot et al., 2000).

Pathologic changes in mineralized dental tissues can result from defects in the apposition and/or mineralization of the tissues (Hu and Simmer, 2007). The larger pulp chambers and reduced amount of dentin in TG mice could be caused by aberrations of matrix production, matrix mineralization, or a combination of the two. Measures of dentin mineralization from uCT scans indicate the dentin mineral density was similar for TG (1201.78±72.22 mg HA/cc) and control (1232.61±94.86 mg HA/cc) teeth, suggesting that the primary dentin defect may affect dentin matrix production rather than its mineralization. Histological analyses and SEM indicate a possible disruption of odontoblast cytodifferentiation in TG mice. Although the orientation, polarity and number of odontoblasts and underlying mesenchyme appeared similar for TG and control littermates in newborn mice (E18.5), by day 14, when the Col1A1 promoter is strongly expressed, odontoblast cytology in TG mice was disrupted. TG teeth have thinner dentin, the normal columnar palisading odontoblast layer is disrupted, and the number of odontoblasts appears to be reduced. As the MT-DLX3 construct utilized a Col1A1 promoter, and Col1A1 is not expressed in odontoblasts until day E17.5 (Sunohara et al., 1996), the temporal nature of these findings coincided with the onset of MT-DLX3 expression in odontoblasts, permitting us to see the effect of MT-DLX3 on odontoblast differentiation (Rossert et al., 1995). At 6 weeks, TG mice show a more severe disruption in odontoblast cytology, the number of odontoblasts appear to be decreased and the thickness of coronal dentin was less than half (TG: 0.084±0.02 mm) that of control teeth (control: 0.217±0.03 mm). In addition to the disruption of odontoblast cytology seen in TG molar and incisor teeth, we noticed the presence of apoptotic bodies which were specific to the odontoblast layer. Therefore, we examined the apoptosis of odontoblasts in vivo and in vitro. The presence of TUNEL-positive and caspase-3-positive cells was restricted to the odontoblast layer of TG mice at 6 weeks, and there was no evidence for apoptosis in alveolar bone cells in TG mice, suggesting cell specificity for apoptosis. In vitro studies demonstrated that expression levels of caspase-3 were increased in odontoblast-like MDPC-23 cells transfected with MT-DLX3, but not in preosteoblastic MC3T3E1 cells, consistent with a differential cell response to MT-DLX3. In addition, apoptotic bodies were not seen in new born or 14-day-old TG mice, and TUNEL staining of first mandibular molars in 14-day-old TG and control mice did not show evidence of apoptosis

(Supplemental Fig. 2), suggesting the aberration in odontoblast cytodifferentiation first seen at 14 days, occurred before the onset of apoptosis. These findings suggested that MT-DLX3 acted primarily on cells of the odontoblast lineage, and appeared to disrupt odontoblast differentiation.

Tooth development can be divided into three overlapping stages: initiation, morphogenesis, and cytodifferentiation (Biz et al., 2010). During the cytodifferentiation stage, odontoblasts become highly complex polarized secretory cells. The differentiation process involves the growth, elongation, and polarization of odontoblasts. Odontoblasts assume a spindle shape characterized by a polarized distribution with the nucleus moving to an apical position and a supra nuclear localization of the organelles, which include a well-developed Golgi apparatus with secretory vesicles and the appearance of a cytoskeleton complex of actin and microtubules (Diekwisch 1989, Magloire et al., 2004, Yamashiro et al., 2007). At the distal end of the cell, a longitudinal arrangement of microtubules forms the primary cilia of odontoblasts which are essential for the secretion of type 1 collagen and dentin matrix proteins such as dentin sialophosphoprotein (DSPP), decorin and biglycan, which form the predentin. Predentin is a fibrillar, unmineralized organic matrix and is converted to mature mineralized dentin by calcium deposition with continuous secretion of dentin matrix proteins from polarized, differentiated odontoblasts. Therefore, differentiation and polarization of odontoblasts are essential to the proper development of predentin and ultimately mature dentin (Thesleff and Mikkola, 2002; Ruch et al., 1995; Magloire et al., 2004; Zhang et al., 2005).

Differentiated odontoblasts are highly polarized secretory cells that are organized as a single layer of tall columnar cells tightly grouped in a palisade arrangement between the dental pulp and the mineralized tubules of dentin. At day 14, odontoblasts in TG mice lacked the ordered columnar appearance seen in control mice, suggesting odontoblast polarization may be defective. Polarization of differentiating ameloblasts and odontoblasts is essential to development of the enamel and dentin (Thesleff and Mikkola, 2002; Zhang et al., 2005; Yamashiro et al., 2007). Epithelial and mesenchymal cells acquire a polarity orthogonal to their apical–basal direction in tooth development. The ameloblastic and odontoblastic tissues polarize within the plane of the epithelial and mesenchymal cell sheet, a process called planar cell polarity (PCP) (Zhang et al., 2005). During this PCP cells expand their cytoplasm, elongate along their apical–basal axis, change cell shape from cuboidal to columnar with apical–basal polarity, and form enamel and dentin forming tissues. The process by which these cells become polarized requires a signaling pathway using Frizzled as a receptor (Axelrod et al., 1998). Responding cells sense cues from their environments that provide directional information, and they translate this information into cellular asymmetry. Although most of what is known about PCP derives from studies in the patterning of the fruit fly wing (Ueno and Greene, 2003), studies of tooth development suggest that planar cell polarity is a key process of odontoblast and ameloblast polarization via various signaling molecules including Wnt10A, Wnt7b, Shh, Dkk, and sFrp (Thesleff and Mikkola, 2002; Zhang et al., 2005). Primary odontoblast cilia are important in molar tooth morphogenesis and ciliopathies have been associated with tooth defects involving disruption of odontoblast polarization in humans and mice, (Prattitichizzo et al., 2008; Thivichon-Prince et al., 2009). Consistent with these results, immunohistochemical study using an acetylated α-tubulin antibody with specificity for the cilia of polarizing odontoblasts demonstrated significant disruption of the odontoblast cilia in TG mice. Cilia are important for dentin tubule formation and proper secretion of dentin matrix proteins (Magloire et al., 2004). Immunohistochemical studies indicated that while the expression patterns of collagen 1A1 and dentin matrix proteins, particularly DSPP, Bgn, and Dcn, are well organized and colocalized with dentinal tubules in control mice, their expression pattern was abnormal in TG mice. Interestingly, in vitro mRNA expression levels of these

proteins were not significantly changed by MT-DLX3 transduction compared to WT-DLX3, suggesting that the basic defect was not in the expression of these gene, but perhaps disruption of odontoblast cytodifferentiation disturbed formation of the dentin tubules and the amount of dentin matrix formed in TG mice. Pavlic et al. (2007) reported disruption of odontoblast differentiation in teeth with taurodontism and hypoplastic amelogenesis imperfecta.

To understand the possible mechanism responsible for the pathologic changes in odontoblast cytodifferentiation, we investigated the expression levels of the odontoblast differentiation and polarization markers Runx2 (Camilleri and McDonald, 2006), Wnt10A (Thesleff and Mikkola, 2002 Yamashiro et al., 2007; Bohring et al., 2009), and TBC1D19 (Zhang et al., 2005). The colocalized expression of DLX3 with *RUNX-2, Wnt10A* and *TBC1D19* in the odontoblast layer suggests that DLX3 may modulate the expressions of these genes in odontoblast differentiation and dentin development. In situ studies indicated that the mRNA expression levels of these genes were reduced in odontoblasts that would be functional in dentin matrix production (Figs. 6d, e, and f), suggesting that down-regulation of these genes may contribute to the abnormal odontoblast polarization, reduced and irregular dentinal tubule formation, and reduced amount of dentin in TG mice. Downregulation of these genes in MT-DLX3 TG mice appears to show specificity for odontoblast cells. In vitro studies also demonstrated that transfection with MT-DLX3 decreased *Runx2* and *Wnt10A* expression odontoblast-like MDPC-23 cells but not in osteoblastic MC3T3E1 cells, consistent with a differential cell response to MT-DLX3. Interestingly, while mRNA expression levels of TBC1D19, an important molecule for the formation of primary cilium polarization (PCP) (Zhang et al., 2005) was reduced in odontoblasts in 6-week-old TG mice, it was not expressed in bone cells (Figs. 6fb and nb). In vitro experiments show that MT-DLX3 directly downregulated TBC1D19 promoter activity and mRNA expression. In addition, siRNA knockdown of the *TBC1D19* gene increased caspase-3 expression more than 90-fold, providing a potential mechanistic link between the perturbed odontoblast polarization and odontoblast apoptosis.

DLX genes are important in establishment of pattern and polarity (Depew et al., 2005), we propose that MT-DLX3 interferes with normal odontoblast cytodifferentiation by disrupting PCP. We further propose that TBC1D19 regulates odontoblast polarization and cilia formation. MT-DLX3-induced disruption of odontoblast cytodifferentiation disrupt normal dentin tubule formation and the ability to form the dentin matrix, leading to production of a thinner dentiin layer and a larger pulp chamber.

These findings led us to hypothesize a mechanism for the reduced dentin development in this TG model whereby (1) the downregulation of TBC1D19 and Wnt10A expression by MT-DLX3 inhibits odontoblast polarization resulted in inhibition of endoplasmic reticulum (ER) development, (2) disrupted secretion and accumulation of dentin matrix proteins in ER causes ER stress, (3) ER stress upregulates caspase-3 expression, and (4) finally increased caspase-3 expression cause odontoblast apoptosis. Consistent with our results, Sasaki and Garant (1996) reported that the differentiation of odontoblasts involves cytoplasmic polarization, the development of the protein synthetic and secretory apparatus, and the active transport of mineral ions. The secretory odontoblast is characterized by the extensive formation of rough-surfaced endoplasmic reticulum (ER) and highly developed Golgi complex. Song et al. (2002) reported that ER stress by inhibiting the ER Ca(2+)-ATPase activates GSK3beta through dephosphorylation of phospho-Ser-9, a prerequisite for caspase-3 activation. Kubota et al. (2005) also reported that exposure to high dose of fluoride on ameloblasts cause endoplasmic reticulum (ER) stress resulted in the caspase-3-mediated apoptosis of ameloblasts.

In summary, findings from this MT-DLX3 TG model expression of MT-DLX3 disrupts planar cell polarization and cilium formation in differentiating odontoblasts, possibly through downregulation of TBC1D19, promoting apoptosis of differentiating odontoblasts. Disruption in odontoblasts differentiation results in a reduced capacity to form dentin matrix and subsequently a smaller amount of mature dentin.

Supplementary Material

Refer to Web version on PubMed Central for supplementary material.

Acknowledgments

We thank Dr. Larry Fisher for DSPP, Bgn, and Dcn antibodies and acknowledge support from the Intramural Program of the NIDCR, National Institutes of Health, Bethesda, MD 20892, USA.

Abbreviations

DLX3	distal less 3
μCT	microcomputed tomography
TDO	tricho-dento-osseous
Col1A1	collagen type1, alpha-1
DSPP	dentin sialophosphoprotein
Bgn	biglycan
Dcn	decorin
Runx2	runt-related transcription factor 2
Wnt10A	wingless-type MMTV integration site family, member 10A
TBC1D19	Tre-2/Bub2/Cdc16 (TBC)1 domain family, member 19
SEM	scanning electron microscopy

References

Assmann KJ, van Son JP, Dijkman HB, Koene RA. A nephritogenic rat monoclonal antibody to mouse aminopeptidase A. Induction of massive albuminuria after a single intravenous injection. J. Exp. Med. 1992; 175:623–635. [PubMed: 1740657]

Axelrod JD, Miller JR, Shulman JM, Moon RT, Perrimon N. Differential recruitment of Dishevelled provides signaling specificity in the planar cell polarity and Wingless signaling pathways. Genes Dev. 1998; 12:2610–2622. [PubMed: 9716412]

Beanan MJ, Sargent TD. Regulation and function of Dlx3 in vertebrate development. Dev. Dyn. 2000; 218:545–553. [PubMed: 10906774]

Biz MT, Marques MR, Crema VO, Moriscot AS, Dos Santos MF. GTPases RhoA and Rac1 are important for amelogenin and DSPP expression during differentiation of ameloblasts and odontoblasts. Cell Tissue Res. 2010 Epub ahead of print.

Bohring A, Stamm T, Spaich C, Haase C, Spree K, Hehr U, Hoffmann M, Ledig S, Sel S, Wieacker P, Röpke A. WNT10A mutations are a frequent cause of a broad spectrum of ectodermal dysplasias with sex-biased manifestation pattern in heterozygotes. Am. J. Hum. Genet. 2009; 85:97–105. [PubMed: 19559398]

Camilleri S, McDonald F. Runx2 and dental development. Eur. J. Oral Sci. 2006; 114:361–373. [PubMed: 17026500]

Choi SJ, Song IS, Ryu OH, Choi SW, Hart PS, Wu WW, Shen RF, Hart TC. A 4 bp deletion mutation in DLX3 enhances osteoblastic differentiation and bone formation in vitro. Bone. 2008; 42:162–171. [PubMed: 17950683]

Choi SJ, Roodman GD, Feng JQ, Song IS, Amin K, Hart PS, Wright JT, Haruyama N, Hart TC. In vivo impact of a 4pb deletion mutation in the DLX3 gene on bone development. Dev. Biol. 2009; 325:129–137. [PubMed: 18996110]

Depew MJ, Simpson CA, Morasso M, Rubenstein JL. Reassessing the Dlx code: the genetic regulation of branchial arch skeletal pattern and development. J. Anat. 2005; 207:501–561. [PubMed: 16313391]

Di Costanzo A, Festa L, Duverger O, Vivo M, Guerrini L, La Mantia G, Morasso MI, Calabrò V. Homeodomain protein Dlx3 induces phosphorylation-dependent p63 degradation. Cell Cycle. 2009; 8:1185–1195. [PubMed: 19282665]

Diekwisch T. Localization of microfilaments and microtubules during dental development in the rat. Acta Histochem. Suppl. 1989; 37:209–212. [PubMed: 2505315]

Duverger O, Lee D, Hassan MQ, Chen SX, Jaisser F, Lian JB, Morasso MI. Molecular consequences of a frameshifted DLX3 mutant leading to tricho-dento-osseous syndrome. J. Biol. Chem. 2008; 283:20198–20208. [PubMed: 18492670]

Feng JQ, Ward LM, Liu S, Lu Y, Xie Y, Yuan B, Yu X, Rauch F, Davis SI, Zhang S, Rios H, Drenzner MK, Quarles LD, Bonewald LF, White KE. Loss of DMP1 causes rickets and osteomalacia and identifies a role for osteocytes in mineral metabolism. Nat. Genet. 2006; 38:1310–1315. [PubMed: 17033621]

Ghoul-Mazgar S, Hotton D, Lézot F, Blin-Wakkach C, Asselin A, Sautier JM, Berdal A. Expression pattern of Dlx3 during cell differentiation in mineralized tissues. Bone. 2005; 37:799–809. [PubMed: 16172034]

Haldeman RJ, Cooper LF, Hart TC, Phillips C, Boyd C, Lester GE, Wright JT. Increased bone density associated with DLX3 mutation in the tricho-dento-osseous syndrome. Bone. 2004; 35:988–997. [PubMed: 15454107]

Hanks CT, Fang D, Sun Z, Edwards CA, Butler WT. Dentin-specific proteins in MDPC-23 cell line. Eur. J. Oral Sci. 1998; 106:260–266. [PubMed: 9541235]

Hassan MQ, Javed A, Morasso MI, Karlin J, Montecino M, van Wijnen AJ, Stein GS, Stein JL, Lian JB. DLX3 transcriptional regulation of osteoblast differentiation: temporal recruitment of MSX2, DLX3, and DLX5 homeodomain proteins to chromatin of the osteocalcin gene. Mol. Cell. Biol. 2004; 24:9248–9261. [PubMed: 15456894]

Hassan MQ, Saini S, Gordon JA, van Wijnen AJ, Montecino M, Stein JL, Stein GS, Lian JB. Molecular switches involving homeodomain proteins, HOXA10 and RUNX2 regulate osteoblastogenesis. Cells Tissues Organs. 2009; 189:122–125. [PubMed: 18701816]

Hu JC, Simmer JP. Developmental biology and genetics of dental malformations. Orthod. Craniofac. Res. 2007; 10:45–52. [PubMed: 17552940]

Hwang J, Mehrani T, Millar SE, Morasso MI. Dlx3 is a crucial regulator of hair follicle differentiation and cycling. Development. 2008; 135:3149–3159. [PubMed: 18684741]

Islam M, Lurie AG, Reichenberger E. Clinical features of tricho-dento-osseous syndrome and presentation of three new cases: an addition to clinical heterogeneity. Oral Surg. Oral Med. Oral Pathol. Oral Radiol. Endod. 2005; 100:736–742. [PubMed: 16301156]

Kubota K, Lee DH, Tsuchiya M, Young CS, Everett ET, Martinez-Mier EA, Snead ML, Nguyen L, Urano F, Bartlett JD. Fluoride induces endoplasmic reticulum stress in ameloblasts responsible for dental enamel formation. J. Biol. Chem. 2005; 280:23194–23202. [PubMed: 15849362]

Lezot F, Thomas B, Hotton D, Forest N, Orestes-Cardoso S, Robert B, Berdal A. Biomineralization, life-time of odontogenic cells and differential expression of the two homeobox genes MSX-1 and DLX-2 in transgenic mice. J. Bone Miner. Res. 2000; 15:430–441. [PubMed: 10750557]

Li H, Marijanovic I, Kronenberg MS, Erceg I, Stover ML, Velonis D, Mina M, Heinrich JG, Harris SE, Upholt WB, Kalajzic I, Lichtler AC. Expression and function of Dlx genes in the osteoblast lineage. Dev. Biol. 2008; 316:458–470. [PubMed: 18280462]

Lu Y, Xie Y, Zhang S, Dusvich V, Bonewald LF, Feng JQ. DMP1-targeted Cre expression in odontoblasts and osteocytes. J. Dent. Res. 2007; 86:320–325. [PubMed: 17384025]

Luukko K, Kvinnsland IH, Kettunen P. Tissue interactions in the regulation of axon pathfinding during tooth morphogenesis. Dev. Dyn. 2005; 2343:482–488. [PubMed: 16217735]

Magloire H, Couble ML, Romeas A, Bleicher F. Odontoblast primary cilia: facts and hypotheses. Cell Biol. Int. 2004; 28:93–99. [PubMed: 14984754]

Martin DM, Hallsworth AS, Buckley T. A method for the study of internal spaces in hard tissue matrices by SEM, with special reference to dentine. J. Microsc. 1978; 112:345–352. J. Cell Biol. 135, 1879-1887. [PubMed: 347084]

Online Mendelian Inheritance in Man, OMIM (TM). Johns Hopkins University; Baltimore, MD: MIM Number: {190320}: {5/14/2008}:World Wide Web URL: http://www.ncbi.nlm.nih.gov/omim/

Pavlic A, Lukinmaa PL, Nieminen P, Kiukkonen A, Alaluusua S. Severely hypoplastic amelogenesis imperfecta with taurodontism. Int. J. Paediatr. Dent. 2007; 17:259–266. [PubMed: 17559453]

Prattichizzo C, Macca M, Novelli V, Giorgio G, Barra A, Franco B. Oral–Facial–Digital Type I (OFDI) Collaborative Group. Mutational spectrum of the oralfacial–digital type I syndrome: a study on a large collection of patients. Hum. Mutat. 2008; 29:1237–1246. [PubMed: 18546297]

Price JA, Bowden DW, Wright JT, Pettenati MJ, Hart TC. Identification of a mutation in DLX3 associated with tricho-dento-osseous (TDO) syndrome. Hum. Mol. Genet. 1998a; 7:563–569. [PubMed: 9467018]

Price JA, Wright JT, Kula K, Bowden DW, Hart TC. A common DLX3 gene mutation is responsible for tricho-dento-osseous syndrome in Virginia and North Carolina families. J. Med. Genet. 1998b; 35:825–828. [PubMed: 9783705]

Rossert J, Eberspaecher H, de Crombrugghe B. Separate cis-acting DNA elements of the mouse pro-alpha 1(I) collagen promoter direct expression of reporter genes to different type I collagen-producing cells in transgenic mice. J. Cell Biol. 1995; 129:1421–1432. [PubMed: 7775585]

Ruch JV, Lesot H, Bègue-Kirn C. Odontoblast differentiation. Int. J. Dev. Biol. 1995; 39:51–68. [PubMed: 7626422]

Sasaki T, Garant PR. Structure and organization of odontoblasts. Anat. Rec. 1996; 245:235–249. [PubMed: 8769666]

Song L, De Sarno P, Jope RS. Central role of glycogen synthase kinase-3beta in endoplasmic reticulum stress-induced caspase-3 activation. J. Biol. Chem. 2002; 277:44701–44708. [PubMed: 12228224]

Sunohara M, Tanzawa H, Kaneko Y, Fuse A, Sato K. Expression patterns of Raf-1 suggest multiple roles in tooth development. Calcif. Tissue Int. 1996; 58:60–64. [PubMed: 8825240]

Thesleff I, Mikkola M. The role of growth factors in tooth development. Int. Rev. Cytol. 2002; 217:93–135. [PubMed: 12019566]

Thesleff I, Vaahtokari A, Kettunen P, Aberg T. Epithelial-mesenchymal signaling during tooth development. Connect. Tissue Res. 1995; 32:9–15. [PubMed: 7554939]

Thivichon-Prince B, Couble ML, Giamarchi A, Delmas P, Franco B, Romio L, Struys T, Lambrichts I, Ressnikoff D, Magloire H, Bleicher F. Primary cilia of odontoblasts: possible role in molar morphogenesis. J. Dent. Res. 2009; 88:910–915. [PubMed: 19783798]

Ueno N, Greene ND. Planar cell polarity genes and neural tube closure. Birth Defects Res. C Embryo Today. 2003; 69:318–324. [PubMed: 14745972]

Weiss KM, Stock DW, Zhao Z. Dynamic interactions and the evolutionary genetics of dental patterning. Crit. Rev. Oral Biol. Med. 1998; 9:369–398. [PubMed: 9825218]

Wright JT, Kula K, Hall K, Simmons JH, Hart TC. Analysis of the tricho-dento-osseous syndrome genotype and phenotype. Am. J. Med. Genet. 1997; 72:197–204. [PubMed: 9382143]

Yamashiro T, Zheng L, Shitaku Y, Saito M, Tsubakimoto T, Takada K, Takano-Yamamoto T, Thesleff I. Wnt10a regulates dentin sialophosphoprotein mRNA expression and possibly links odontoblast differentiation and tooth morphogenesis. Differentiation. 2007; 75:452–462. [PubMed: 17286598]

Zhang YD, Chen Z, Song YQ, Liu C, Chen YP. Making a tooth: growth factors, transcription factors, and stem cells. Cell Res. 2005; 15:301–316. [PubMed: 15916718]

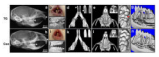

Fig. 1.

Appearance, high resolution radiography, and μCT analysis of teeth from 6-week-old male mice (a–g: TG mice; h–n: control mice). Panels a, c, h, and j: high-resolution radiography; panels b and i: photography; panels d–g and panels k–n: μCT. Panels d and k: show optical sectioning of mandibular transverse views; panels e and l show optical sections of maxillary transverse views. Panels f and m show cusp patterns of maxillary molars. Panels g and n show transverse two dimensional sections of mandibular molars with mesial and distal dentin thickness indicated by red lines. Reduced dentin thickness was seen in both molars and incisors of TG mice as compared to comparable control teeth (indicated by white arrowheads in TG teeth in panels a, c, d, and e).

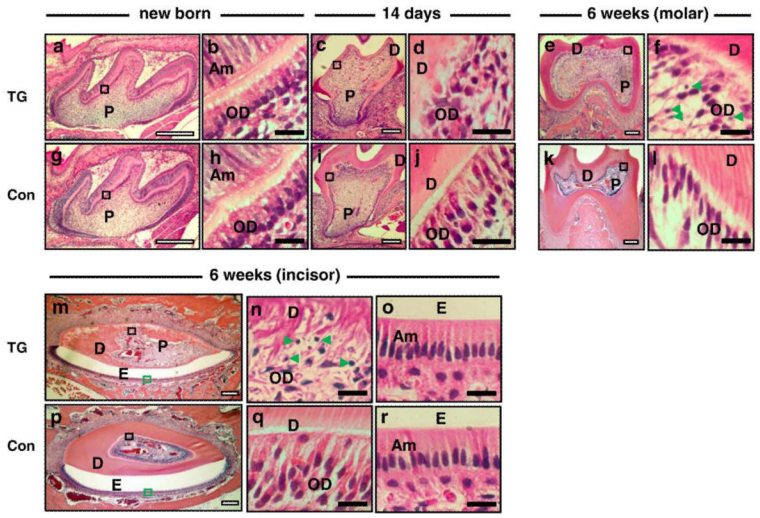

Fig. 2.

Histological analysis of mandibular first molars (newborn, 14 days, and 6 weeks) and mandibular incisors (6 weeks) from TG and control mice. H&E staining was performed on tooth sections (a–f and m–o: TG mice and g–l and p–r: control mice). Panels a, b, g, and h: mandibular first molars of new born mice; panels c, d, i, and j: mandibular first molars of 14-day-old mice; panels e, f, k, and l: mandibular first molars of 6-week-old mice. Panels m–r: mandibular incisors of 6-week-old mice. Panels b, d, f, h, j, l, n, and q: high-power magnification of odontoblasts from the area inside the black box shown in the low magnification images. Panels o and r are high-power magnification of ameloblasts from the green rectangular box shown in the low-power images m and p, respectively (D: dentin; E: enamel; P: pulp; OD: odontoblast layer; Am: ameloblast layer). Apoptotic bodies are seen in mandibular first molar and mandibular incisor teeth sections of 6-week-old TG mice as indicated with green arrow heads (f and n). White scale bars are 100 μm, and black scale bars are 10 μm.

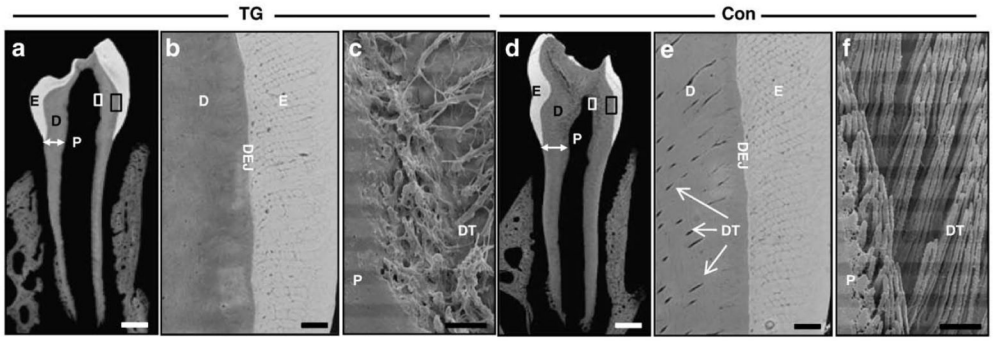

Fig. 3.

Dentin and enamel microstructure of mandibular first molars from TG (a–c) and control (d–f) mice. Coronal section of mandibular first molars by backscattered (a, b, d, and e) and resin cast (c and f) scanning electron microscopy. High-power magnification of dentin–enamel junction (DEJ) areas for TG (panel b) and control (panel e) teeth, where the enlarged areas are indicated by black rectangular boxes in the lower-power panels a and d, respectively. High-power magnification of the pulp and dentin junction area are shown for TG (panel c) and control (panel f) teeth with the magnified areas indicated by white rectangular box in the respective panels a and d (D: dentin; E: enamel; P: pulp; DT: dentinal tubule; DEJ: dentin-enamel junction; white arrows in panel a and d show dentin width). The thickness of mineralized dentin and the number of dentinal tubules are reduced in the TG mouse mandibular first molar. White scale bars are 200 μm, and black scale bars are 10 μm.

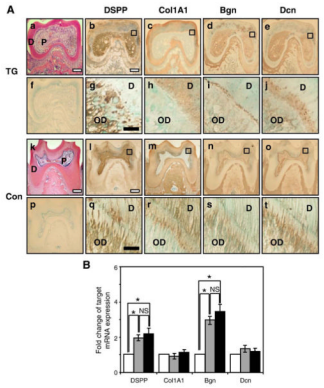

Fig. 4.

(A) Expression patterns of dentin matrix proteins in mandibular first molars from 6-week-old mice (a–j: TG mice; and k–t: control mice). Panels a and k: H&E staining; panels f and p: prebleeding rabbit anti sera; panels b, g, l, and q show DSPP antibody; panels c, h, m, and r show collagen type I-αI (Col1A1) antibody; panels d, i, n, and s show biglycan (Bgn) antibody; and panels e, j, o, and t show decorin (Dcn) antibody. Panels g, h, i, j, q, r, s, and t show high-power magnification of the dentin from the black box areas indicated in the respective lower-power panels above (OD: odontoblast layer; D: dentin; P: pulp). White scale bars are 100 μm, and black scale bars are 10 μm. (B) mRNA expression levels of the dentin matrix proteins, DSPP, Col1A1, Bgn, and Dcn, by real-time RT–PCR from odontoblast-like MDPC-23 cells transfected with empty vector (white bars), WT-DLX3 (grey bars), and MT-DLX3 (black bars) (**P*<0.05; NS: not significantly different).

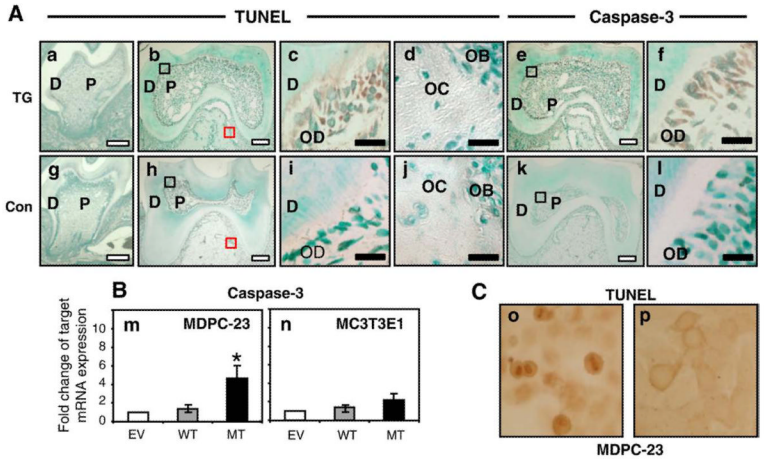

Fig. 5.

(A) Increased apoptosis in differentiated odontoblasts from 6-week-old mandibular first molar TG teeth sections. Panel a: mandibular first molar section of 14-day-old TG mouse; panel g: mandibular first molar section of 14-day-old control mouse. Panels b–f: mandibular first molar sections of 6-week-old TG mouse; panels h–l: mandibular first molar sections of 6-week-old control mouse. Panels a–d and panels g–j show TUNEL staining with panels c and i showing high-power magnifications of the dentin and odontoblast layers and panels d and j showing magnification of alveolar bone (magnified areas are indicated with black boxes (dentin) and red boxes (bone) in panels b and h respectively). Panels e, f, k, and l show caspase-3 staining, with panels f and l showing magnification of dentin from areas indicated by black boxes in panels e and k, respectively (D: dentin; P: pulp; OD: odontoblast; OB: osteoblast; OC: osteocyte). Apoptosis is increased in the differentiated odontoblasts in tooth dentin but not in cells from alveolar bone from TG mice. White scale bars are 100 μm, and black scale bars are 10 μm. (B) mRNA expression levels of caspase-3 in odontoblast-like MDPC-23 (m) and preosteoblastic MC3T3E1 (n) cells stably transfected with empty vector (EV: white bar), WT-DLX3 (grey bar), and MT-DLX3 (black bar) cDNA at day 3. Similar results were seen in three independent experiments. Means±SD are presented (**P*<0.05). (C) TUNEL staining of odontoblast-like MDPC-23 cells transfected with MT-DLX3 (o) and WT-DLX3 (p) at day 5.

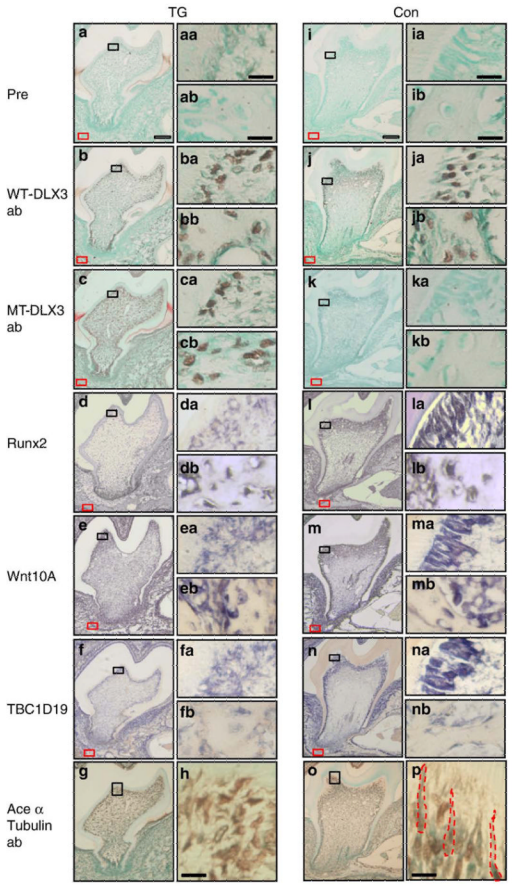

Fig. 6.

Expression patterns of WT-DLX3, MT-DLX3, and acetylated α-tubulin proteins and Runx2, Wnt10A, and TBC1D19 mRNA in the mandibular first molars of 14-day-old mice (a–h: teeth sections of TG mouse; i–p: teeth sections from control mouse). Panels a and i show prebleeding rabbit antisera; panels b and j show WT-DLX3-specificantibody; panels c and k show MT-DLX3-specific antibody; panels d and l show Runx2 in situ hybridization; panels e and m show Wnt10A in situ hybridization; panels f and n show TBC1D19 in situ hybridization; panels g, h (high-power magnification), o, and p (high-power magnification) show acetylated α-tubulin antibody. Panels aa–na show high-power magnification of differentiated odontoblasts from the black rectangular box seen in the respective low-power panels. Panels ab–nb show high-power magnification of osteoblasts of the alveolar bone from the areas indicated by a red rectangular box in the respective low-power panels. Higher-power magnification of acetylated α-tubulin staining show primary ciliary morphology of odontoblasts in control mice (red dot line in panel p) but not in TG mouse (h). White scale bars are 100 μm, and black scale bars are 10 μm.

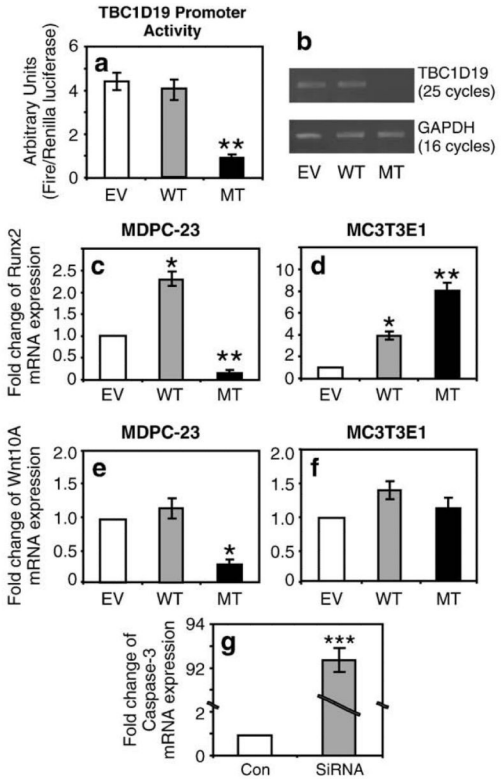

Fig. 7.

Effects of MT-DLX3 on Runx2, Wnt10A, TBC1D19, and caspase-3 mRNA expression in odontoblast-like MDPC-23 and preosteoblastic MC3T3E1 cells. Transfection of MT-DLX3 into odontoblast-like MDPC-23 cells significantly decreases TBC1D19 promoter activity (a) and mRNA expression (b) (EV = empty vector; WT = wild type DLX3; MT = mutant DLX3). MT-DLX3 expression significantly reduces Runx2 expression in MDPC-23 cells (c) and significantly increases Runx2 expression in MC3T3E1 cells (d). MT-DLX3 expression significantly reduces Wnt10A expression in MDPC-23 cells (e) but does not significantly changes Wnt10A expression in MCT3T3E1 cells (f). Transfection of siRNA against TBC1D19 increases caspase-3 mRNA expression more than 90-fold (g). Similar results were seen in three independent experiments. Means±SD are presented (**P*<0.05, ***P*<0.005, ****P*<0.0005).